Fill and dump measurement of the neutron lifetime using an asymmetric magneto-gravitational trap

C. Cude-Woods,[1,2] F. M. Gonzalez,[3,4,5] E. M. Fries,[6] T. Bailey,[1] M. Blatnik,[6] N. B. Callahan,[7] J. H. Choi,[1,2] S. M. Clayton,[8] S. A. Currie,[8] M. Dawid,[3,4] B. W. Filippone,[6] W. Fox,[3,4] P. Geltenbort,[9] E. George,[10] L. Hayen,[1,2] K. P. Hickerson,[6] M. A. Hoffbauer,[8] K. Hoffman,[10] A. T. Holley,[10] T. M. Ito,[8] A. Komives,[11] C.-Y. Liu,[1,2] M. Makela,[8] C. L. Morris,[8,*] R. Musedinovic,[1,2] C. O'Shaughnessy,[8] R. W. Pattie, Jr.,[12] J. Ramsey,[5] D. J. Salvat,[3,4] A. Saunders,[8,5] E. I. Sharapov,[13] S. Slutsky,[6] V. Su,[6] X. Sun,[6] C. Swank,[6] Z. Tang,[8] W. Uhrich,[8] J. Vanderwerp,[3,4] P. Walstrom,[8] Z. Wang,[8] W. Wei,[6] and A. R. Young[1,2]

[1]*Department of Physics, North Carolina State University, Raleigh, North Carolina 27695, USA*
[2]*Triangle Universities Nuclear Laboratory, Durham, North Carolina 27708, USA*
[3]*Department of Physics, Indiana University, Bloomington, Indiana 47405, USA*
[4]*Center for Exploration of Energy and Matter, Indiana University, Bloomington, Indiana 47405, USA*
[5]*Oak Ridge National Laboratory, Oak Ridge, Tennessee 37831, USA*
[6]*Kellogg Radiation Laboratory, California Institute of Technology, Pasadena, California 91125, USA*
[7]*Argonne National Laboratory, Lemont, Illinois 60439, USA*
[8]*Los Alamos National Laboratory, Los Alamos, New Mexico 87545, USA*
[9]*Institut Laue-Langevin, CS 20156, 38042 Grenoble Cedex 9, France*
[10]*Tennessee Technological University, Cookeville, Tennessee 38505, USA*
[11]*DePauw University, Greencastle, Indiana 46135, USA*
[12]*East Tennessee State University, Johnson City, Tennessee 37614, USA*
[13]*Joint Institute for Nuclear Research, 141980 Dubna, Russia*

(Received 6 May 2022; accepted 17 November 2022; published 26 December 2022)

The past two decades have yielded several new measurements and reanalysis of older measurements of the neutron lifetime. These have led to a 4.4 standard deviation discrepancy between the most precise measurements of the neutron decay rate producing protons in cold neutron beams and the most precise lifetime measured in neutron storage experiments. Measurements using different techniques are important for investigating whether there are unidentified systematic effects in any of the measurements. In this paper we report a new measurement using the Los Alamos asymmetric magneto-gravitational trap where the surviving neutrons are counted external to the trap using the fill and dump method. The new measurement gives a free neutron lifetime of $\tau_n = 876.3(2.4)_{\text{stat}}(0.8)_{\text{syst}}$. Although this measurement is not as precise, it is in statistical agreement with previous results using *in situ* counting in the same apparatus.

DOI: 10.1103/PhysRevC.106.065506

I. INTRODUCTION

The unitarity of the Cabibbo-Kobayashi-Maskawa matrix, which describes the weak mixing among the six flavors of quarks, provides a stringent test of the standard model of particle physics. Recent analysis of the current status of the unitarity test suggests strong evidence for discrepancies in the unitarity for couplings to the up quark [1] and highlights the impact of unitarity constraints on the possible origin of a shift in the mass of the W particle [2].

The first row is most easily measured because the dominant matrix element V_{ud} can be inferred from nuclear (including neutron) β decay measurements. Neutron decay has the potential to provide V_{ud} to a precision exceeding that achieved in nuclear β decay because of smaller uncertainties due to the simpler structure of the neutron [3–7]. However, the current data set [8–20] shows a large discrepancy in lifetimes obtained by measuring the rate of neutron decay resulting in protons in the final state [14] and neutron lifetimes measured by counting surviving neutrons stored in a trap experiments [21]. A disputed [22] independent analysis of systematic uncertainties in the beam experiment [23] suggests that charge exchange on residual gas was not sufficiently analyzed in the beam experiment and that this effect might explain the discrepancy, but this needs to be tested. Measurements using different techniques that might identify systematic uncertainties that have not been identified are necessary to confirm or eliminate this discrepancy.

In this paper we present new data taken using the asymmetric magneto-gravitational ultracold neutron (UCN) trap [24] that was used for recently reported lifetime measurements [16,18,20] but using a different counting technique. Rather than *in situ* "dagger" detector counting we have unloaded the neutrons and counted them external to the trap, the so-called fill and dump technique.

*Corresponding author: cmorris@lanl.gov

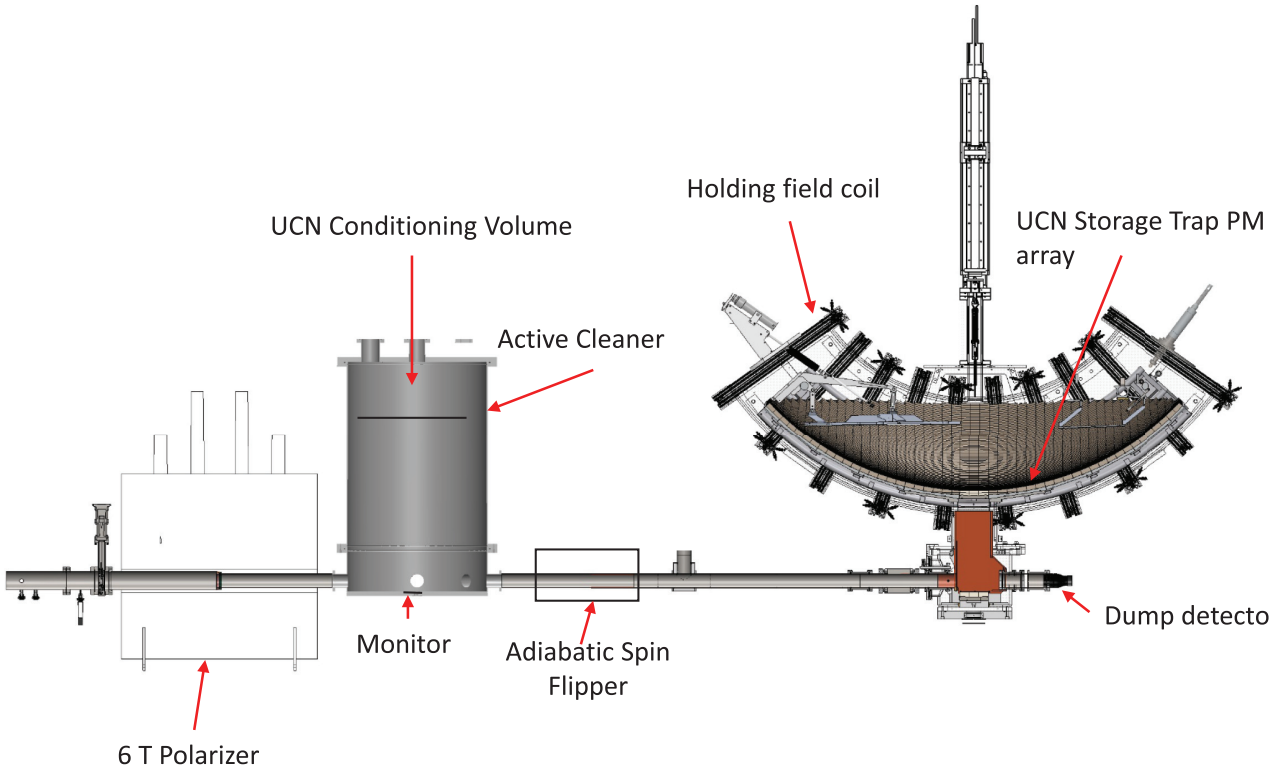

FIG. 1. Experimental layout showing the location of the UCN detectors used in this experiment. The source is off the picture to the left. The dump detector is the primary counter for this experiment.

II. EXPERIMENT

The Los Alamos Ultracold Neutron Facility produces a high density of (UCNs by down-scattering spallation neutrons produced using pulsed 800-MeV protons from the Los Alamos Neutron Science Center accelerator at the Los Alamos National Laboratory (LANL) incident on a solid deuterium (SD_2) converter [25,26]. These neutrons are transported using nickel phosphorous- (NiP-) coated guides [27,28] through a 6-T prepolarizing superconducting solenoid magnet (PPM) that selects high-field-seeking UCN and an adiabatic spin flipper that converts them to low-field-seeking UCN. The lower part of the source is coated with ^{58}Ni with a Fermi potential of 335 neV [28]. Neutrons exiting the SD_2 receive a 108-neV boost because of the Fermi potential of the solid. A 1-m rise before a 4-m long horizontal chicane in the guide system removes the boost, resulting in a spectrum from the source with maximum energy of 230 neV. This is reduced to 213 neV by the potential of the NiP guide. This is further reduced by a section of stainless-steel guide between the shielding wall and the PPM to 186 neV. The source vacuum that contains SD_2 is isolated from the experiment by a 50-μm aluminum foil at the center of the PPM that allows a vacuum on the order of 10^{-7} torr to be maintained downstream despite $10^{-4}-$torr pressure spikes in the source due to beam heating of the source. The magnetic potential of the PPM of 360 neV ensures high transmission through the embedded aluminum foil which has a potential of $\approx$ 54 neV as well has high spin polarization of the transmitted UCN.

The low-field-seeking neutrons are loaded into the magnetic trap by removing a small section of the Halbach array, the "trap door" (see Fig. 1). The neutrons are stored in the trap by replacing the trap door. In the previous work [20], those stored UCN were counted in place by lowering a ^{10}B-coated ZnS detector [29] into the trap. This provided a variable counting time of a few seconds, depending on the thickness of the ^{10}B coating and minimized errors introduced by the coupling between the phase space of the UCN and the time at which the UCNs are counted. A detailed discussion of phase-space evolution in this trap is given by Callahan *et al.* [30].

Here we report a set of measurements performed using the same experimental apparatus with the same UCN loading procedures but with the neutrons counted at the end of storage by unloading through the trap door into an external detector. The time constant for counting UCN in a dagger with a 20-nm ^{10}B coating lowered to the bottom of the trap is 7.1(2) s. The time constant for unloading UCN in this experiment is 26.8(8) s. Although these experiments share many sources of systematic uncertainties, the coupling between phase-space evolution and counting could be much larger in this experiment because of the longer unloading time. These results provide a test of the method used to estimate the size of this systematic uncertainty in the previous experiment.

In Fig. 1 UCNs enter from the left. The 6-T magnetic field in the polarizing magnet selects only high-field-seeking UCN. UCNs then pass through the adiabatic fast passage spin flipper [31] where they are converted into low-field-seeking UCN. A large buffer volume serves to filter out fluctuations

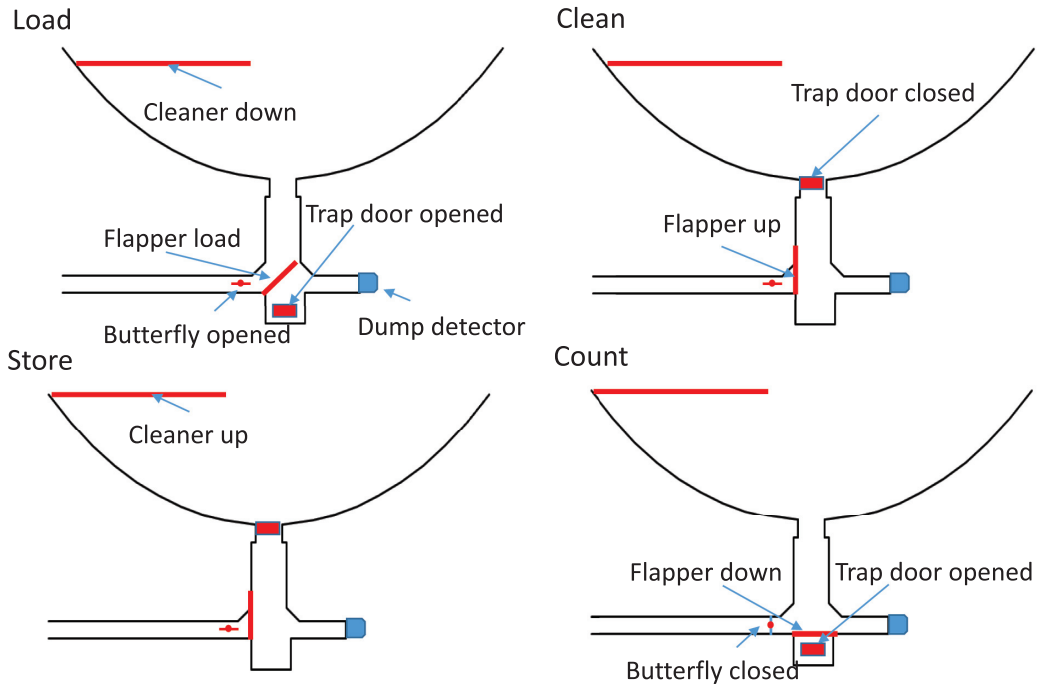

FIG. 2. Schematic showing the valve configurations for loading, cleaning, storing, and counting. The valve changes for each step are labeled.

in the beam intensity due to the proton beam delivery, and an active cleaner removes and counts neutrons with velocities too high to be trapped. The active cleaner and monitor in the buffer volume are used to normalize the experiment as will be described below. A coil provides a holding field of $\approx$ 10 G in the buffer volume.

The trap [24] is formed of vertically oriented toroids, one with a minor radius of 1.0 m and a major radius of 0.5m, the other with a major radius of 0.5 m and a minor radius of 1.0 m. These mated on the axis where the surfaces of both toroids had radii of 1.5 m. The torii are cut off at 50 cm above their lowest point and are contained in a vacuum jacket. The surface of the toroids was made from rows of neodymium boron iron permanent magnets arranged as a Halbach array. The minimum field at the surface of the toroids was about 0.8 T, providing a trapping potential for low-field-seeking UCN of 48 neV.

A set of window-frame copper coils outside of the permanent-magnet bowl trap provided a holding field parallel to the Halbach array surface, thereby eliminating field zeroes and depolarization in field zeroes (see Fig. 1). The strength of the holding field varied from 60 to 120 G, depending on the position in the trap.

A cleaner whose surface was a combination of polyethylene and ^{10}B/ZnS was lowered to a level of 38 cm above the bottom of the trap to remove high-energy UCN, well below the upper edge of the trap, and was raised to 50 cm for the storage period. This ensured that the remaining population was trapped. The fraction of untrapped UCN after cleaning was previously measured and found to be small [20]. The time constant for removing high-energy neutrons was measured to be 8 s.

The sequence of loading, storing, and counting the UCN is shown in Fig. 2. The sequence was controlled by three valves, the flapper, butterfly, and trap door. The trap door is a section of magnets that can be lowered to open a hole in the bottom of the trap. The flapper had three positions: an up position, used to raise and lower the trap door; a 45° position, to optimize transport into the trap; and a down position, to minimize UCN interactions with the lowered trap door when unloading the trapped UCN. The butterfly valve located upstream of the loading port was open for loading and closed for counting. The trap door was lowered for loading and counting and raised to store UCN in the trap.

The UCN detector was composed of a 76-mm diameter photomultiplier tube viewing a 120-nm-thick ^{10}B/ZnS detector [29]. The diameters were chosen to collect a large fraction of the light and to fill the inside diameter of the guide with an active surface. The ^{10}B/ZnS was inside of the vacuum, and the light was transported to the photomultiplier via a Lucite light pipe that also served as the vacuum window. The Fermi potential of the 10B i (−4 neV) and its thickness (120 nm) give high efficiency for detection of UCN. The signals were processed using a timing filter amplifier, which integrated for 100 ns, and a single channel analyzer (MSC4 from FAST ComTec Communication Technology GmbH). These were then counted in a multichannel multiscalar that also recorded the monitor signals as a function of time.

III. ANALYSIS

The results presented here were obtained from 189 runs taken over a week of running. Data were taken in run sequences (octets) that included holding times of 20, 1550,

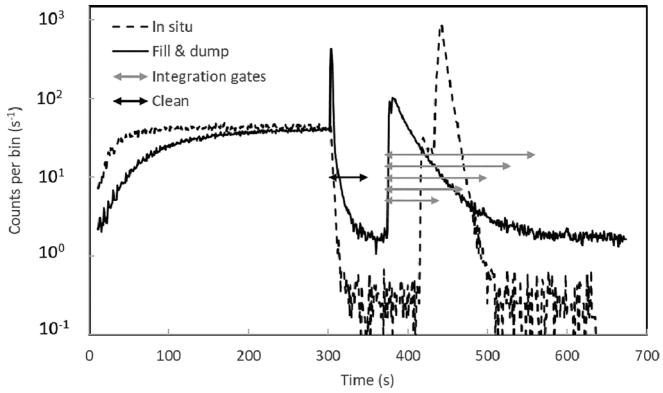

FIG. 3. Counting spectrum in fill and dump mode (solid) and *in situ* counting (dashed). The unloading times are 28 and 7 s for fill and dump and *in situ* counting, respectively. The integration gates for fill and dump are shown as the solid gray double arrows. The double peak in the *in situ* counting curve is because UCNs were counting at two different dagger positions. The loading curves are different because of the different counter positions.

1550, 50, 100, 1550, 1550, and 200 s, a sequence designed to cancel normalization drifts. A spectrum from a 20-s holding time run is shown in Fig. 3 where counting for fill and dump is compared to *in situ* counting. The spike and decay at the end of filling is due to the emptying of the guides as the trap door closes, and the flapper moves to its up position. This process takes about 4 s. The ≈1.5 Hz background is attributed to thermal neutrons interacting in the ^{10}B, cosmic ray, and Compton electron produced Cherenkov light in the rather massive Lucite light pipe. The UCN counting rate in the fill and dump detector during counting (between 0 and 300 s in Fig. 3) is due to leakage of UCN through the flapper valve whereas it is in its 45 ° "filling" position, meant to guide the UCNs into the trap. We speculate that the slower buildup time in the fill and dump detector than in the *in situ* (dagger) detector during filling, visible between 0 and ≈ 200 s in Fig. 3, is due to the very different energy spectra of the UCNs sampled by those detectors during the filling period. The *in situ* detector is about 1 m higher than the fill and dump detector. Consequently, the UCN detected in the *in situ* detector have higher average velocities in the bulk of the transport from the source than those leaked into the fill and dump detector and, thus, reach equilibrium more quickly. Qualitatively, we see a similar effect when comparing the round house monitor detector with the round house cleaner detector. The cleaner detector reaches equilibrium much faster than the monitor detector because it is higher and detects neutrons that have higher energy during the transport process.

Yields Y_{0k} and uncertainties ΔY_{0k} were calculated for each run k as

$$Y_{0k} = \frac{S_k - B_k}{N_k},$$
$$\Delta Y_{0k} = \frac{\sqrt{S_k + B_k}}{N_k}, \qquad (1)$$
$$N_k = \sum_i a_i \mathrm{RHAC}_i,$$

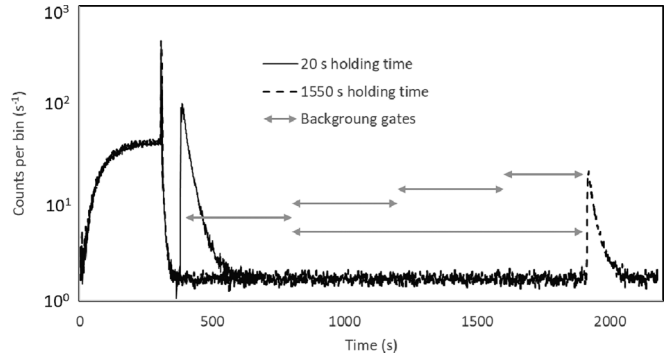

FIG. 4. The figure shows a comparison of the average of the short holding time runs with the long holding time runs. The gray double arrows show the background gates that have been used in the analysis.

where S_k is the sum of counts in a 130-s-long counting gate beginning at the time the trap door is opened, B_k is the background obtained from a nearby long holding time run (see Fig. 4). The normalization N_k was calculated using the counting rate during the fill from the round house active cleaner (RHAC_i), which was binned into 25-s-long groups. These were summed with weights for each group a_i that were optimized to reduce the sensitivity of the yields to beam fluctuations. The weights were fixed at values obtained by fitting a larger independent data set taken with *in situ* counting.

The background counting rate was obtained from the long holding time runs, which had a long background region from the end of cleaning to the beginning of counting. Backgrounds for the short holding time runs were obtained from the nearest-subsequent long holding time runs. This background analysis was performed after unblinding the data because of concerns about the lack of a background region in the short holding time runs. It resulted in a shift in the lifetime 1.2 s from the initial background analysis, which used a run-by-run region at the end of counting, which still included some stored UCNs. The new method provided a longer region and reduced statistical uncertainty in the background estimates.

This normalization is based on the higher velocity part of the spectrum with energies above the trapping potential. Degradation of the surface of the solid deuterium of the source results in both reduced output and hardening of the UCN spectra [32]. These time-dependent normalization changes were accounted for by using a linear correction based on the ratio of the round house monitor (RHMON) to the round house active cleaner (RHAC) detector (see Fig. 1).

The nonzero corrections were applied to the yields,

$$Y_k = \frac{Y_{0k}}{1 - b(r_k - \bar{r}_k)},$$
$$\Delta Y_k = \frac{\Delta Y_{0k}}{1 - b(r_k - \bar{r}_k)}, \qquad (2)$$
$$r_k = \frac{\mathrm{RHMON}}{\mathrm{RHAC}}.$$

The constant b was obtained fitting the same independent data set used to get a_i. The average value of the correction,

$1-b(r_k - \bar{r}_k)$ was 1.00, the total variation across the data set was 0.08, and the root mean square was 0.05. The neutron lifetime is introduced using a correction factor (CF) calculated using the neutron lifetime τ and the holding time t_k,

$$Y_{\mathrm{calc},k} = e^{-(t_k/\tau)},$$
$$R_k = \frac{Y_k}{Y_{\mathrm{calc},k}},$$
$$\mathrm{CF} = \bar{R}_k. \tag{3}$$

The UCN source output changes due to the exact geometry of the solid deuterium source. To keep the source output high, the deuterium crystal must be reformed approximately every 2 to 3 days. The average normalization factor CFis taken over surrounding short runs (holding times of 20, 50, 100, and 200 s) with discrete breaks to account for these source rebuilds. This procedure removes any remaining long-term drifts without the need for complete octets. This leads to a larger useful data set because accelerator failures in the early filling stage, leading to excluded bad runs, were common.

The ΔY_k were assumed to have a Gaussian distribution. The neutron lifetime is obtained by fitting τ to minimize the χ^2,

$$\chi^2 = \sum_k \frac{(Y_k - Y_{\mathrm{calc},k}\mathrm{CF}_k)^2}{(\Delta Y_k)^2}, \tag{4}$$

where the statistical uncertainties in the normalization factor were scaled up by about a factor of 3 to account for fluctuations not captured by the counting uncertainties. Incorporating the round house was shown to reduce these additional fluctuations by ≈ 2, but the loading time constants for loading, pulse-to-pulse variations in the primary beam current, and local fluctuations in the pressure above the source can all lead to uncertainties in the normalization not captured by counting statistics or by the corrections described above. Without this factor the reduced X^2 was 1.2. This is consistent with previous observations [20]. The counting uncertainties were assumed to have a Gaussian distribution. Here, the number of degrees of freedom df is one less than the number of yields. The statistical uncertainty in the lifetime is taken as the change in τ needed to increase the X^2 by 1.

Variations in the width of the foreground integration gate and the location of the background region (shown in Figs. 3 and 4) were studied to establish a system systematic error associated with the background subtraction. The lifetime was taken as an average over these tests (shown in Fig. 5), and a systematic uncertainty due to the background model was taken as the standard deviation of these values.

The yields measured here, in the fill and dump mode, were only 32% of those measured through *in situ* counting. Transport into and out of the trap is known to be lossy. This is the result of gaps in the guides leading into the trap and depolarization in the complicated field structure with the trap door removed, which we speculate leads to spin flip and neutron loss as neutrons move in and out of the trap.

There is a bias in the lifetime due to the assumption of Gaussian statistics. The bias arises because larger counts have higher weights in a calculated mean. This effect is larger at longer times because of the lower average count and higher variance relative to shorter holding times. This correction is larger here than in Ref. [20] because of the lower UCN counts. This biases the fitted lifetime to be longer than the actual lifetime. Three different methods were used to account for this bias in the high-precision measurements [20]. Here, the bias was estimated by Monte Carlo. A large number of datasets were generated and fitted to obtain lifetimes with known parent lifetimes as a function of the number of initial neutrons. The difference between the fitted and the actual lifetimes was the statistical bias. This was tabulated as a function of the initial count and used to calculate the correction on a run-by-run basis. The net correction is −0.71 s with negligible uncertainty.

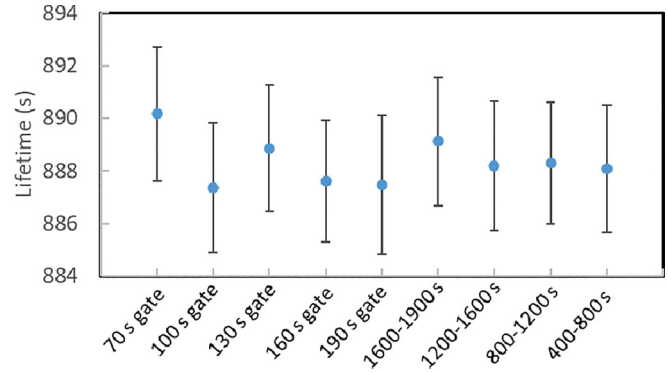

FIG. 5. Data points are the results of the background systematic study. The first five points, labeled with the foreground gate width, used a background region of 400–1600 s. In the last four points the background region was varied with the foreground gate width fixed at 130 s.

The nominal holding times were used in the fit. The mean counting time can be affected by evolution of the UCN phase space during storage in the trap because different regions of phase space can have different unloading times. The difference in the change of the actual (determined from the mean arrival time) and nominal holding times between long and short holding time runs was found to be 0.28 ± 0.26 s leading to a shift in the lifetime of -0.17 ± 0.15 s as shown in Table I.

TABLE I. Systematic uncertainties and corrections to the neutron lifetime are given in seconds. The uncleaned, heated, depolarization, and normalization systematic uncertainties were taken from Ref. [20].

Effect	Correction	Uncertainty
Uncleaned		0.11
Heated		0.08
Residual gas scattering		0.10
Depolarization		0.07
Dead time correction	−0.02	0.02
Phase-space evolution	−0.17	0.15
Background model		0.85
Normalization		0.06
Uncorrelated sum		0.89

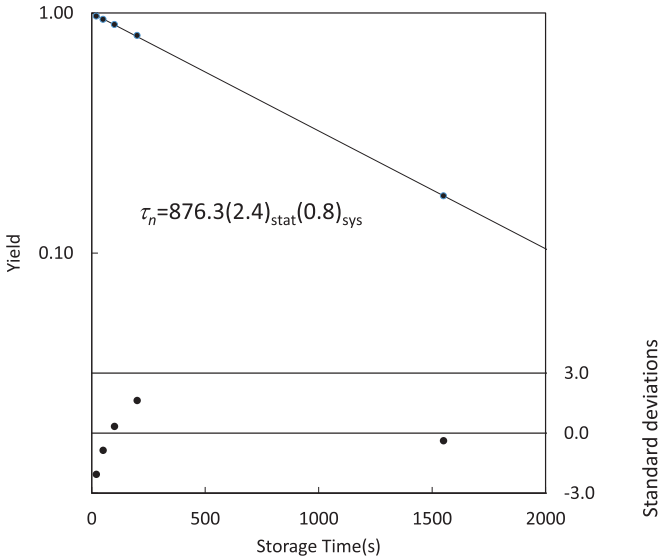

FIG. 6. Plot of average yield vs time, lifetime fit, and residuals.

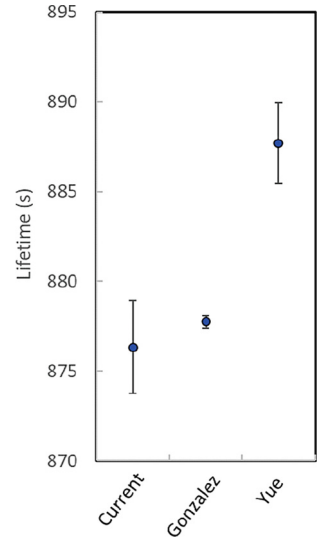

FIG. 7. Comparison of the most precise beam [20] and trap lifetimes [14] along with the current result. The plotted uncertainties are the quadratic sum of the statistical and systematic uncertainties for each measurement.

This compares to a much smaller value of 0.01–0.03 s in Ref. [20].

The pressure in the trap was monitored with a cold cathode vacuum gauge. A correction to the lifetime was computed based on these pressures averaged across the dataset and the cross sections reported in Refs. [33,34]. The residual gas was assumed to be dominated by water; an assumption supported by previous mass spectrometer measurements.

A summary of the systematic uncertainties is given in Table I.

Some of the corrections still included some stored (dead time, phase-space evolution, and residual gas correction) and the background analysis were applied after unblinding the data. The average yields as a function of holding time along with the lifetime fit is shown in Fig. 6). We find $\tau_n = 876.3(2.4)_{\text{stat}}(0.8)_{\text{syst}}$s, where the first uncertainty is statistical and the second is systematic. Figure 5 compares the most precise beam (Yue) [14] and trap lifetime measurements (Gonzalez) [20] with the current result. A χ^2 test gives the probability (assuming Gaussian statistics) of the previous beam and trap measurement being consistent of 1.2×10^{-5}, the current result and the beam result of 9×10^{-4}, and the current result and the trap result of 0.6. This measurement does not identify any discrepancy in the measurement of Gonzalez *et al.* [20] (in Fig. 7) that can help to resolve the difference between the beam and the trap results.

IV. CONCLUSIONS

The neutron lifetime in the Los Alamos magneto-gravitational trap measured using the fill and dump method agree with those using *in situ* counting in the same trap. This very different counting method has many disadvantages when compared to *in situ* counting but is potentially sensitive to unidentified systematic uncertainties in *in situ* counting. However, we have not identified any new systematic errors that can explain the 4.4 standard deviation difference between the beam and the trap results associated with the counting method.

ACKNOWLEDGMENTS

This work was supported by the LANL LDRD Program; the U.S. Department of Energy, Office of Science, Office of Nuclear Physics under Awards No. DE-FG02-ER41042, No. DE-AC52-06NA25396, No. DE-AC05-00OR2272, and No. 89233218CNA000001 under proposal LANLEDM; NSF Grants No. 1614545, No. 1914133, No. 1506459, No. 1553861, No. 1812340, No. 1714461, No. 2110898, and No. 1913789; and a NIST precision measurements Grant.

[1] V. Cirigliano *et al.*, Semileptonic tau decays beyond the Standard Model, J. High Energy Phys. 04 (2022) 152.

[2] V. Cirigliano, W. Dekens, J. de Vries, E. Mereghetti, and T. Tong, Beta-decay implications for the W-boson mass anomaly, Phys. Rev. D **106**, 075001 (2022).

[3] A. Czarnecki, W. J. Marciano, and A. Sirlin, Radiative corrections to neutron and nuclear beta decays revisited, Phys. Rev. D **100**, 073008 (2019).

[4] M. Gorchtein and C.-Y. Seng, Dispersion relation analysis of the radiative corrections to gA in the neutron β-decay, J. High Energy Phys. 10 (2021) 053.

[5] J. C. Hardy and I. S. Towner, 13th Conference on the Intersections of Particle and Nuclear Physics, Palm Springs, California, USA (2018), arXiv:1807.01146.
[6] C.-Y. Seng, M. Gorchtein, and M. J. Ramsey-Musolf, Dispersive evaluation of the inner radiative correction in neutron and nuclear β decay, Phys. Rev. D **100**, 013001 (2019).
[7] L. Hayen, Standard model O (α) renormalization of g A and its impact on new physics searches, Phys. Rev. D **103**, 113001 (2021).
[8] W. Mampe *et al.*, Measuring neutron lifetime by storing ultracold neutrons and detecting inelastically scattered neutrons, Sov. J. Exp. Theor. Phys. Lett. **57**, 82 (1993).
[9] J. Byrne *et al.*, A revised value for the neutron lifetime measured using a Penning trap, Europhys. Lett. **33**, 187 (1996).
[10] A. Serebrov *et al.*, Measurement of the neutron lifetime using a gravitational trap and a low-temperature Fomblin coating, Phys. Lett. B **605**, 72 (2005).
[11] A. Pichlmaier *et al.*, Neutron lifetime measurement with the UCN trap-in-trap MAMBO II, Phys. Lett. B **693**, 221 (2010).
[12] S. Arzumanov *et al.*, Analysis and correction of the measurement of the neutron lifetime, JETP Lett. **95**, 224 (2012).
[13] A. Steyerl *et al.*, Quasielastic scattering in the interaction of ultracold neutrons with a liquid wall and application in a reanalysis of the Mambo I neutron-lifetime experiment, Phys. Rev. C **85**, 065503 (2012).
[14] A. Yue *et al.*, Improved Determination of the Neutron Lifetime, Phys. Rev. Lett. **111**, 222501 (2013).
[15] S. Arzumanov *et al.*, A measurement of the neutron lifetime using the method of storage of ultracold neutrons and detection of inelastically up-scattered neutrons, Phys. Lett. B **745**, 79 (2015).
[16] C. Morris *et al.*, A new method for measuring the neutron lifetime using an in situ neutron detector, Rev. Sci. Instrum. **88**, 053508 (2017).
[17] V. Ezhov *et al.*, Measurement of the neutron lifetime with ultracold neutrons stored in a magneto-gravitational trap, JETP Lett. **107**, 671 (2018).
[18] R. Pattie, Jr. *et al.*, Measurement of the neutron lifetime using a magneto-gravitational trap and in situ detection, Science **360**, 627 (2018).
[19] A. Serebrov *et al.*, Neutron lifetime measurements with a large gravitational trap for ultracold neutrons, Phys. Rev. C **97**, 055503 (2018).
[20] F. Gonzalez *et al.*, Improved Neutron Lifetime Measurement with UCN τ, Phys. Rev. Lett. **127**, 162501 (2021).
[21] G. L. Greene and P. Geltenbort, The neutron enigma, Sci. Am. **314**, 36 (2016).
[22] F. Wietfeldt *et al.*, A Comment on "The possible explanation of neutron lifetime beam anomaly" by AP Serebrov *et al.*, arXiv:2004.01165.
[23] A. Serebrov *et al.*, Search for explanation of the neutron lifetime anomaly, Phys. Rev. D **103**, 074010 (2021).
[24] P. Walstrom *et al.*, A magneto-gravitational trap for absolute measurement of the ultra-cold neutron lifetime, Nucl. Instrum. Methods Phys. Res. Sect. A **599**, 82 (2009).
[25] A. Saunders *et al.*, Demonstration of a solid deuterium source of ultra-cold neutrons, Phys. Lett. B **593**, 55 (2004).
[26] T. M. Ito *et al.*, Performance of the upgraded ultracold neutron source at Los Alamos National Laboratory and its implication for a possible neutron electric dipole moment experiment, Phys. Rev. C **97**, 012501 (2018).
[27] Z. Tang *et al.*, Measurement of spin-flip probabilities for ultracold neutrons interacting with nickel phosphorus coated surfaces, Nucl. Instrum. Methods Phys. Res. Sect. A **827**, 32 (2016).
[28] R. W. Pattie Jr. *et al.*, Evaluation of commercial nickel–phosphorus coating for ultracold neutron guides using a pinhole bottling method, Nucl. Instrum. Methods Physi. Res., Sect. A **872**, 64 (2017).
[29] Z. Wang *et al.*, A multilayer surface detector for ultracold neutrons, Nucl. Instrum. Methods Phys. Res., Sect. A **798**, 30 (2015).
[30] N. Callahan *et al.*, Monte Carlo simulations of trapped ultracold neutrons in the UCN τ experiment, Phys. Rev. C **100**, 015501 (2019).
[31] V. Luschikov and Y. V. Taran, On the calculation of the neutron adiabatic spin-flipper, Nucl. Instrum. Methods Phys.ics Res., Sect. A **228**, 159 (1984).
[32] A. Anghel *et al.*, Solid deuterium surface degradation at ultracold neutron sources, Eur. Phys. J. A **54**, 148 (2018).
[33] S. Seestrom *et al.*, Upscattering of ultracold neutrons from gases, Phys. Rev. C **92**, 065501 (2015).
[34] S. J. Seestrom *et al.*, Total cross sections for ultracold neutrons scattered from gases, Phys. Rev. C **95**, 015501 (2017).